



Cortical development in fetuses with congenital heart defects using an automated brain-age prediction algorithm

Journal:	<i>Acta Obstetrica et Gynecologica Scandinavica</i>
Manuscript ID	AOGS-19-0358.R1
Wiley - Manuscript type:	Original Research Article
Date Submitted by the Author:	14-Jun-2019
Complete List of Authors:	<p>Everwijn, Sheila; Leiden University Medical Center, Obstetrics Namburete, Ana; University of Oxford, Institute of biomedical engineering van Geloven, Nan; Leiden Universitair Medisch Centrum Jansen, Fenna; Leiden University Medical Center, Obstetrics and fetal therapy Papageorgiou, Aris ; John Radcliffe Hospital, Obstetrics and Gynecology Noble, Alison; University of Oxford Teunissen, Aalbertine; Leiden Universitair Medisch Centrum, Obstetrics Rozendaal, Lieke; Leiden University Medical Center, Pediatric Cardiology Blom, Nico; Leids Universitair Medisch Centrum, Pediatric Cardiology van Lith, Jan; Leiden University Medical Center, Obstetrics and Fetal therapy Haak, Monique; Leiden University Medical Center, Obstetrics and fetal therapy</p>
Keywords:	Prenatal diagnosis, Ultrasound

SCHOLARONE™
Manuscripts

1
2
3 **1 Cortical development in fetuses with congenital heart defects using an**
4 **automated brain-age prediction algorithm**
5
6
7

8
9
10 4 Sheila M. P. Everwijn¹; Ana I. L. Namburete²; Nan van Geloven³, Fenna A. R. Jansen¹, Aris
11 5 T. Papageorgiou⁴, Alison J. Noble², Aalbertine K. K. Teunissen¹, Lieke Rozendaal⁵, Nico
12 6 A. Blom⁵, Jan M. M. van Lith¹, Monique C. Haak¹
13
14
15
16
17

18 8 1 Department of Obstetrics and Prenatal Diagnosis, Leiden University Medical Center,
19 9 Leiden, Netherlands

20
21
22 10 2 Institute of Biomedical Engineering, Department of Engineering Science, University of
23 11 Oxford, Oxford, UK

24
25
26 12 3 Department of Biomedical Data Sciences, Section Medical Statistics, Leiden University
27 13 Medical Center, Leiden, Netherlands

28
29
30 14 4 Nuffield Department of Obstetrics and Gynecology, John Radcliffe Hospital, University of
31 15 Oxford, UK

32
33
34 16 5 Department of Pediatric Cardiology, Leiden University Medical Center, Leiden,
35 17 Netherlands
36
37
38
39
40
41

42 **19 Corresponding Author:**

43
44
45 20 Sheila Maria Pieternella Everwijn

46
47 21 Leiden University Medical Center, Department of Obstetrics – prenatal diagnosis and fetal
48 22 therapy K6-P, Postbus 9600, 2300 RC Leiden , The Netherlands

49
50
51 23 E-mail: s.m.p.everwijn@lumc.nl
52
53

54
55
56 25 **Conflict of interest**

57
58
59 26 None
60

1
2
3 27
4
56 **28 Funding**
7

8 29 The authors received no specific funding for the completion of this work. ATP is supported
9 30 by the Oxford Partnership Comprehensive Biomedical Research Centre with funding from
10 31 the NIHR Biomedical Research funding scheme.
11
12

13
14 32
15
16
17
18
19
20
21
22
23
24
25
26
27
28
29
30
31
32
33
34
35
36
37
38
39
40
41
42
43
44
45
46
47
48
49
50
51
52
53
54
55
56
57
58
59
60

For Peer Review

ABSTRACT

Introduction: Congenital heart defects are associated with neurodevelopmental delay. It is hypothesized that fetuses affected by congenital heart defect have altered cerebral oxygen perfusion and are therefore prone to delay in cortical maturation. The aim of this study was to determine the difference in fetal brain age between consecutive congenital heart defect cases and controls in the second and third trimester using ultrasound. **Material and methods:** Since 2014, we have included 90 isolated severe congenital heart defect cases in the Heart And Neurodevelopment(HAND)-study. Every four weeks, detailed neurosonography was performed in these fetuses, including the recording of a 3D volume of the fetal brain, from 20 weeks onward. 75 healthy fetuses underwent the same protocol to serve as a control group. The volumes were analyzed by automated age prediction software which determines gestational age by the assessment of cortical maturation. **Results:** In total 477 volumes were analyzed using the age prediction software (199 volumes of 90 congenital heart defect cases; 278 volumes of 75 controls). 16 (3.2%) volume recordings were excluded because of imaging quality. The age distribution was 19-33 weeks. Mixed model analysis showed that the age predicted by brain maturation was 3.0 days delayed compared to the control group ($p = 0.002$). **Conclusions:** This study shows that fetuses with isolated cases of congenital heart defects show some delay in cortical maturation as compared to healthy control cases. The clinical relevance of this small difference is debatable. This finding was consistent throughout pregnancy and did not progress during the third trimester.

Keywords:

Congenital Heart Defects, Malformations of cortical development,| Ultrasonography, Fetus, Neurodevelopmental outcome

Key Message:

Fetuses with congenital heart defects are shown to have a slight delay in cortical maturation when compared to controls, using a novel brain-age prediction algorithm.

1
2
3 **63 Abbreviations**
4

5
6 **64 CHD** congenital heart defect
7

8 **65 MRI** magnetic resonance imaging
9

10
11 **66 GA** gestational age
12

13 **67 POF** parieto-occipital fissure
14

15
16 **68 SF** sylvian fissure
17

18
19 **69**

20
21 **70**
22

23
24 **71**
25
26
27
28
29
30
31
32
33
34
35
36
37
38
39
40
41
42
43
44
45
46
47
48
49
50
51
52
53
54
55
56
57
58
59
60

For Peer Review

73 INTRODUCTION

74 Improvements over time in the quality of neonatal care and cardiothoracic surgery in children
75 with congenital heart defects (CHD) have resulted in an increased survival of children with
76 severe CHD. This has stimulated longer term follow up and a recognition that there is an
77 association between CHD and impaired neurodevelopmental outcome.^{1,2} Developmental
78 delay, decreased IQ and behavioral disorders have been reported, even in non-syndromic
79 CHD children.¹

80 Previously, these sequelae were attributed to perioperative hypoxia or thrombo-embolic
81 events during surgery. Recent studies suggest, however, that signs of abnormal neurological
82 development may be present prior to surgery.³⁻⁵ Imaging studies in pregnancy using magnetic
83 resonance imaging (MRI)^{6,7} and ultrasound^{8,9}, have shown signs of delayed fetal brain
84 development. It has been suggested that it is these abnormal findings that result in the altered
85 neurological outcome later in life.^{5,6} The hypothesized mechanism is that the abnormal
86 development of the brain is the result of altered brain oxygenation in fetal life.^{10,11}

87 However, there is no robust evidence for delayed fetal brain maturation, because the current
88 studies are subject to potential bias due to the small number of included affected women and
89 due to selection of participants with regard to the type of cardiac defect.⁴

90 Therefore, the aim of this study is to assess fetal brain development and maturational changes
91 over time in a prospective, consecutive cohort of fetuses with isolated CHD, to avoid
92 selection bias. In this study, ultrasound (US) imaging was used, this not only enables the
93 inclusion of a larger number of fetuses (and thus reduces selection bias), but also facilitates
94 multiple examinations in the same fetus, to evaluate brain development and changes over
95 time. Furthermore, the used technique assesses brain maturation automatically and is
96 therefore blinded, which, in combination with repeated measurements, are important
97 differences with previous studies.

98 We hypothesize that the patterns of brain maturation of fetuses with CHD are delayed
99 compared to control fetuses.

100

101 MATERIAL AND METHODS

102

103 **Data acquisition**

104 All consecutive pregnant women, diagnosed with a fetal CHD before 32 weeks gestation at
105 the Leiden University Medical Center between March 2014 and December 2016, were
106 approached to participate in the Heart And Neurodevelopment (HAND)-study. To account
107 for natural variation of cortical development in the healthy population, we constructed a
108 control group by the recruitment of unselected pregnant women after a normal structural
109 anomaly scan. Control cases were not offered additional genetic testing but had a postnatal
110 visit in which dysmorphic features were assessed. Gestational age (GA) in both the CHD
111 cases and the control cases, was based on first-trimester ultrasound at approximately 10
112 weeks gestation, according to Dutch national guidelines. For both cases and controls we
113 excluded: Maternal age <18 years, multiple gestation, genetic or syndromic defects
114 (prenatally diagnosed or postnatally apparent up to the age of six months), cases with
115 placental pathology (pre-eclampsia, severe growth restriction) and cases that showed normal
116 cardiac anatomy after birth. In the CHD group, non-isolated cases were excluded. The
117 reasons for only including isolated CHD was that altered neurodevelopment could otherwise
118 be attributed to genetic or syndromic defects. Furthermore, cases with aortic valve stenosis
119 that underwent fetal balloon valvuloplasty were excluded, since fetal brain oxygenation may
120 have changed due to the intervention during pregnancy.¹² Also, strictly minor cases
121 (persistent left caval vein, mild pulmonary stenosis and restrictive foramen ovale) were also
122 excluded, since in these cases, blood flow towards the brain is expected to be
123 uncompromised. The sample size calculation for the normal reference population was based
124 on the available evidence from two MRI-studies^{7, 13} that compared hypoplastic left heart
125 syndrome (HLHS)-fetuses to controls, to detect a difference in mean brain age of two weeks.
126 The normal reference population was calculated to consist of 60 fetuses. The CHD-group
127 contains all the women that met the inclusion criteria and were referred between March 2014
128 – December 2016.

129 A CHD in combination with minor associations – namely a single umbilical artery; enlarged
130 first-trimester nuchal translucency with normal chromosomal analysis and small for GA with
131 normal Doppler recordings, were considered as isolated CHD. These cases were not excluded
132 unless genetic syndromes became apparent postnatally.

133 A detailed neurosonographic examination was performed in cases and controls every four
134 weeks after the diagnosis or in the case of controls after normal standard anomaly scan.

1
2
3 135 Examinations were undertaken by experienced sonographers (FJ/AT/SE) using a RAB 6-D
4 136 three-dimensional transducer on a Voluson E8 or E10 (GE Healthcare ultrasound,
5 137 Milwaukee, WI, USA). The examination was conducted transabdominally in four scanning
6 138 planes: axial, coronal, sagittal and parasagittal. At these visits, we assessed the presence of
7 139 structural brain anomalies and fetal biometry. Multiple 3D volume recordings were obtained
8 140 in the axial plane, starting at head circumference level of the transthalamic plane. The 3D
9 141 acquisition was performed in the maximum quality setting (6-12 seconds) or on high quality
10 142 setting (2-8 seconds) to limit the amount of movement artefacts.
11
12
13
14
15
16
17
18

13

19 144 **Brain-Age prediction algorithm**

20
21
22 145 The evaluation of brain maturation by 2D ultrasound imaging is known to have an agreeable
23 146 rate of inter-observer variation. Data from recent MRI studies show a strong correlation
24 147 between the degree of gyrification and GA^{14, 15}, neuropathologists consider the appearance
25 148 and stage of the sulci to be so precise¹⁴ that cortical complexity can be used as an accurate
26 149 proxy for intrauterine neurodevelopment. Therefore, we used a semi-automated age
27 150 prediction algorithm as a proxy for cortical maturation. At each visit a mean of 2.7(0.9) 3D
28 151 volumes for cases and 3.5(1.2) for controls were recorded. These volume recordings were
29 152 examined to identify cases with poor acquisition quality due to fetal motion artifacts. The
30 153 recording with the highest quality was selected to enter into the algorithm. All 3D volumes
31 154 were processed with a study-code, which did not reveal the presence of a heart defect or not.
32 155 Plane localization was annotated manually in each 3D volume using the ITK-SNAP tool.¹⁶
33 156 The algorithmic details on the process of predicting brain maturation from a 3D ultrasound
34 157 volume were previously described.¹⁷ Briefly, a 3D surface-based coordinate system is
35 158 spatially aligned to the cranial pixels in the image. This coordinate system allows for the
36 159 sampling of brain regions based on surface locations. The US image and its corresponding
37 160 surface are passed into a regression forest model, where they traverse the nodes of a set of
38 161 pre-trained binary decision trees, within the forest. At each node, a binary test is applied to a
39 162 sampled brain region to evaluate whether it is indicative of a more or less advanced stage of
40 163 maturation. In this way, each brain region (eg callosal sulcus, thalamic region, cingulate
41 164 sulcus, parieto-occipital fissure (POF), sylvian fissure (SF), central sulcus and ventricular
42 165 regions) votes for a particular brain age (figure 1). The final prediction of brain maturation is
43 166 achieved by averaging the votes from the brain regions, across the full set of decision trees in
44 167 the forest. Thus, the algorithm is able to estimate the brain-age according the pattern of

1
2
3 168 gyrification of the fetal cortex, which varies during gestation (figure 2). Furthermore, since
4
5 169 the true GA was known for each case, we were able to compare the brain-age with the true
6
7 170 age to determine any delay in cortical maturation. A more extensive description of the
8
9 171 algorithm is available as Supporting information Appendix S1.

10 11 172 **Data handling**

12
13 173 The prenatal diagnosis was compared to the postnatal echocardiographic findings. In case of
14
15 174 discrepancy, the postnatal diagnosis or the results of post mortem examination in case of
16
17 175 pregnancy termination, were considered as the definitive cardiac diagnosis. In cases in which
18
19 176 the parents did not give consent for post mortem examination, the prenatal diagnosis was
20
21 177 used for this study. We have previously shown that the rate of discrepancies is low in our
22
23 178 unit.¹⁸

24 25 179 **Statistical analyses**

26
27 180 We investigated evidence of the presence of systematic between-group differences in brain
28
29 181 age, as calculated by the age prediction algorithm, between the CHD group and the control
30
31 182 group. We have selected the data from measurements at 19 – 33 weeks since the age
32
33 183 prediction algorithm had been validated in this GA.¹⁷

34
35 184 As multiple volume measurements were acquired from the same patient during pregnancy
36
37 185 (longitudinal repeated-measures data) linear mixed modeling must be applied to account for
38
39 186 systematic within-patient correlation. The mixed-effect regression model corrected for GA
40
41 187 (assumed to relate linearly to the age prediction), group (CHD-cases vs controls) and the
42
43 188 interaction between GA and group as fixed effects. Within-patient correlation was modeled
44
45 189 by inclusion of a random-effect intercept per individual. The presence of a between-group
46
47 190 difference was then assessed by removing both the interaction term and the main group effect
48
49 191 from the full model and assess the associated likelihood ratio test with two degrees of
50
51 192 freedom. As the likelihood ratio test confirmed the presence of group effect, two follow-up
52
53 193 hypothesis tests were investigated. Firstly, the main group difference was assessed at the
54
55 194 median GA by comparing the (marginal) mean brain-age in that set. Secondly, regression
56
57 195 slopes were compared between CHD-cases and controls to assess whether groups differed in
58
59 196 their maturation speed. In a sensitivity analysis we repeated the tests allowing for a quadratic
60
197 effect of GA. All statistical analysis were performed using IBM SPSS statistics version
198
199 24.0.0.0 (IBM, Armonk, NY, USA). Statistical significance was determined when $p \leq 0.05$.

199 **Ethical Approval**

200 This study was approved by the local ethics committee on March 17, 2014 under ref. number
201 P13.107.

202

203 **RESULTS**

204 In the study period, 90 consecutive CHD cases and 75 controls were included (see Table 1 for
205 study characteristics). The groups were not prospectively matched for baseline
206 characteristics, however the groups did not differ significantly in maternal age, parity, body
207 mass index or maternal diabetes. We excluded 14 cases according the defined exclusion
208 criteria, of which eight were postnatal diagnoses of genetic syndromes (three CHARGE
209 syndrome, two Kabuki syndrome, three with postnatal multiple dysmorphic features, final
210 genetic diagnosis pending). The genetic diagnosis of the CHD-cases was followed up until
211 one year postnatally. 30 % of control cases opted for first-trimester screening. No genetic or
212 structural abnormalities were found in the control-group up to six months postnatally. Thus, a
213 total of 152 CHD cases and controls were eligible for analysis. From these 152 women, in
214 493 scanning sessions, volume recordings were made. Of these volumes, 16 (3.2%) were
215 excluded due to ultrasonographic factors (oblique insonation, fetal movement artifacts or very
216 poor image quality), resulting in 477 volumes suitable for analysis by the age-prediction
217 algorithm. In total, 199 volumes in 77 cases (mean of 2.4 recorded volumes per woman) and
218 278 volumes in 75 controls (mean of 3.7 recorded volumes per woman) were analyzed using
219 the automated age prediction algorithm. The CHD cases were scanned at 1-5 different time
220 points during pregnancy, with 63% of the women scanned more than once. For the control
221 group, all cases were measured more than once.

222 The fetal brain-age of the healthy control cases was calculated by the age prediction
223 algorithm. This cohort of normal fetuses showed a calculated brain-age by the algorithm
224 which did not statistically differ from the true GA ¹⁷, based on first-trimester ultrasound
225 suggesting the model is applicable to our cohort. The predicted brain-age increased perfectly
226 linear in the second trimester and the algorithm tends to slightly underestimate the brain age
227 during the third trimester (figure 3).

228 The overall test indicated that the time trend significantly differed between CHD-cases and
229 controls ($p=0.005$) indicating that indeed there was a group effect. When comparing CHD

1
2
3 230 cases with controls, the brain-age determined by the algorithm was lower compared to
4
5 231 controls at the median true GA (26.20 vs 26.61 weeks; difference 3.0 days, 95% CI (1.07 to
6
7 232 4.63) $p = 0.001$. (figure 4) The speed of the development of the brain maturation (i.e. slopes
8
9 233 of the curves), between both groups did not differ statistically significant. Cortical maturation
10
11 234 was estimated to increase with 4.45 vs 4.52/days per week ($p = 0.78$) for CHD cases and
12
13 235 controls, indicating similar speed of maturation between CHD cases and controls. This was
14
15 236 also analyzed with a quadratic age trend analysis, which confirmed the similar increase in
16
17 237 cortical maturation between cases and controls.
18
19 238

20 239 **DISCUSSION**

21
22
23 240 In this study of a consecutive cohort of fetuses with isolated CHD fetuses, we found a delay
24
25 241 in fetal brain-age of 3.0 days, compared to normal fetuses. The delay was continuous
26
27 242 throughout our study period, which opposes the earlier findings that suggest further delay in
28
29 243 cortical maturation with advancing gestation.^{7, 19} This study is the first to implement a
30
31 244 validated automated algorithm to assess fetal cortical development using ultrasound, to a
32
33 245 clinically relevant group.

34 246 Neurodevelopmental delay in CHD children has been recognized for decades, even with
35
36 247 optimized pre-operative and neonatal care.²⁰ prenatal brain damage is hypothesized to result
37
38 248 from the altered hemodynamics caused by the cardiac defect, which may result in decreased
39
40 249 flow or oxygenation of the blood directed towards the brain^{21, 22}, resulting in delayed brain
41
42 250 development. Increased N-acetylaspartate to choline (NAA:Cho)-ratio and increased lactate
43
44 251 levels in MRI and spectroscopy studies support a decrease in brain oxygenation in the
45
46 252 developing fetal brain of fetuses with CHD.^{19, 23}

47 253 Cortical maturation by measuring fissure depth has been described before using both MRI¹⁴
48
49 254 and US^{24, 25} in non-CHD fetuses, application of these techniques show significant differences
50
51 255 in the depth of the POF and Calcarine fissure in CHD cases as compared to controls.⁶⁻⁹ These
52
53 256 fissures were also reported to be shallower in CHD neonates when compared to controls with
54
55 257 a comparable GA³, which was explained as delayed maturation. The findings in these studies
56
57 258 are, however, not in full agreement with each other. A significant decrease in depth of the SF,
58
59 259 POF and Calcarine fissure was found by some authors⁸ whereas others did not find a
60
260 significant difference in the SF depth⁶, but did find an overall decrease in brain maturation.⁹

1
2
3 261 The differences in the results of these studies can be explained by the small sample sizes,
4 262 different methodologies, and the differences in statistical analysis of the data.⁹
5
6

7 263 Our study is the first to convey the development of cortical maturation with ultrasound by
8 264 using maturational age as an outcome measure. Thus, the used methodology in this study is
9 265 capable to determine the extent of the delay, which was demonstrated to be small (3.0 days).
10
11 266 Moreover, we do not see a difference in the slopes of the development between CHD and
12 267 control cases, indicating no further delay in the cortical growth trajectory in the third
13 268 trimester, as described by other authors.^{7,9} A possible explanation for this absence of third
14 269 trimester difference, might be that the role of fetal brain oxygenation is being magnified in
15 270 literature due to case selection. Decreased head growth as a proxy for brain development and
16 271 developmental delay has however also been demonstrated in other types of CHDs which
17 272 suggest a role for placental, genetic or epigenetic factors.
18
19

20
21 273 A common method of assessing fetal cortical development in the previously mentioned
22 274 studies is a manual, sometimes unblinded, measurement of the depth of two-three fissures.⁶⁻⁹
23 275 The applied algorithm in our study automatically selects the most age-discriminating regions
24 276 of the entire fetal brain. As cortical maturation is an excellent proxy for brain age, this does
25 277 not imply that the sulcation in itself is a linear phenomenon.^{14,26} The sampled locations (eg
26 278 callosal, cingulate and central sulcus, thalamic region, POF and SF) are proven as the most
27 279 distinct points to assess maturation speed, as the algorithm used automated deep learning in a
28 280 large cohort of normal fetuses.¹⁷ It is therefore arguable if the maturation patterns of the
29 281 commonly chosen fissures in previous studies (SF, POF and calcarine fissure) are sensitive
30 282 enough to detect brain maturation and representative of the global cortical development, as
31 283 our algorithm selected more sulci to be able to assess brain-age with a precision of 6 days.¹⁷
32
33

34 284 Another important difference with previous studies is the fact that we included cases with
35 285 isolated CHD and have excluded neonates that were diagnosed with genetic syndromes
36 286 (routinely tested with micro-array or whole exome sequencing) after birth. Although previous
37 287 studies report the exclusion of aneuploid fetuses⁶⁻⁸, only de Koning et al.⁹ report the postnatal
38 288 exclusion of syndromic cases. Since a significant amount of genetic syndromes present with
39 289 mental retardation, abnormal brain development could be caused not solely by the CHD in
40 290 itself.
41
42

43
44
45
46
47
48
49
50
51
52
53
54
55
56
57
58 291 Whether a delay of three days is clinically relevant, is debatable. On the other hand one could
59 292 argue that even though differences are small, they could still have an impact on long term
60

1
2
3 293 outcome, since the detected delay is visible in early life.²⁷ Two of the studies mentioned
4
5 294 above^{6, 8} found significant differences when correlating cortical maturation and
6
7 295 neurodevelopmental outcome by performing Bayley Scales of Infant and Toddler
8
9 296 Development (BSID). However, authors performed BSID in a minority of infants and,
10
11 297 paradoxically, only in milder CHD cases. With this sparse evidence, it is undisputable that
12
13 298 there is an urgent need to explore the relation between altered fetal brain maturation and
14
15 299 neurodevelopmental outcome further. As this is a limitation of the current study, we are
16
17 300 planning to correlate the findings in this cohort to postnatal neurodevelopment.

18 301 It is controversial which imaging modality is superior to detect abnormalities in fetal brain
19
20 302 development. While we do acknowledge the fact that MRI is regarded as the gold standard
21
22 303 for detecting structural brain abnormalities²⁸, both previously mentioned MRI-studies only
23
24 304 comprise a single MRI acquisition during pregnancy, with slice thicknesses of 1,5-3 mm,
25
26 305 which will influence the accuracy of the measurements as well. We believe that repeated
27
28 306 measurements by US in the hands of experienced sonographers is sensitive enough to study
29
30 307 brain maturation trajectories.

31 308 A limitation of this study is the assessment of all CHD-cases combined. We acknowledge
32
33 309 that fetuses with lower oxygen delivery to the brain might be prone to delayed cortical
34
35 310 development, reduced head circumference and brain lesions.^{10, 19, 22, 29} However, reduced head
36
37 311 circumference, as a proxy for brain development, has been reported in fetuses with only a
38
39 312 single ventricular septal defect.³⁰ We have chosen to not stratify according to CHD, as the
40
41 313 current group is too small to make statements on cortical development. Stratification
42
43 314 according lesion physiology will be possible in the future as we continue monitoring these
44
45 315 cases.

46 316 A second limitation is the upper GA limit of included cases, because brain visibility is
47
48 317 obscured due to acoustic shadowing and fetal position in the late third trimester.

49 318

50 51 52 319 **CONCLUSION**

53
54
55 320 This study shows that fetuses with isolated cases of CHDs show some delay in cortical
56
57 321 maturation as compared to healthy control cases. The clinical relevance of this small
58
59 322 difference is debatable. This finding was consistent throughout pregnancy and did not
60
323 progress during the third trimester.

324 **REFERENCES**

- 325 1. Marino BS, Lipkin PH, Newburger JW, et al. Neurodevelopmental outcomes in children with
326 congenital heart disease: evaluation and management: a scientific statement from the American Heart
327 Association. *Circulation*. 2012;126(9):1143-72.
- 328 2. Paladini D, Alfirevic Z, Carvalho JS, et al. ISUOG consensus statement on current
329 understanding of the association of neurodevelopmental delay and congenital heart disease: impact on
330 prenatal counseling. *Ultrasound Obstet Gynecol*. 2017;49(2):287-8.
- 331 3. Licht DJ, Shera DM, Clancy RR, et al. Brain maturation is delayed in infants with complex
332 congenital heart defects. *J Thorac Cardiovasc Surg*. 2009;137(3):529-36; discussion 36-7.
- 333 4. Jansen FA, Everwijn SM, Scheepjens R, et al. Fetal brain imaging in isolated congenital heart
334 defects - a systematic review and meta-analysis. *Prenat Diagn*. 2016;36(7):601-13.
- 335 5. Majnemer A, Limperopoulos C, Shevell MI, Rohlicek C, Rosenblatt B, Tchervenkov C. A
336 new look at outcomes of infants with congenital heart disease. *Pediatr Neurol*. 2009;40(3):197-204.
- 337 6. Masoller N, Sanz-Cortes M, Crispi F, et al. Mid-gestation brain Doppler and head biometry in
338 fetuses with congenital heart disease predict abnormal brain development at birth. *Ultrasound Obstet
339 Gynecol*. 2016;47(1):65-73.
- 340 7. Clouchoux C, du Plessis AJ, Bouyssi-Kobar M, et al. Delayed cortical development in fetuses
341 with complex congenital heart disease. *Cereb Cortex*. 2013;23(12):2932-43.
- 342 8. Peng Q, Zhou Q, Zang M, et al. Reduced fetal brain fissures depth in fetuses with congenital
343 heart diseases. *Prenat Diagn*. 2016;36(11):1047-53.
- 344 9. Koning IV, van Graafeiland AW, Groenenberg IAL, et al. Prenatal influence of congenital
345 heart defects on trajectories of cortical folding of the fetal brain using three-dimensional ultrasound.
346 *Prenat Diagn*. 2017;37(10):1008-16.
- 347 10. Sun L, Macgowan CK, Sled JG, et al. Reduced fetal cerebral oxygen consumption is
348 associated with smaller brain size in fetuses with congenital heart disease. *Circulation*.
349 2015;131(15):1313-23.
- 350 11. Al NB, van Amerom JF, Forsey J, et al. Fetal circulation in left-sided congenital heart disease
351 measured by cardiovascular magnetic resonance: a case-control study. *J Cardiovasc Magn Reson*.
352 2013;15:65.
- 353 12. Prosnitz AR, Drogosz M, Marshall AC, et al. Early hemodynamic changes after fetal aortic
354 stenosis valvuloplasty predict biventricular circulation at birth. *Prenat Diagn*. 2018;38(4):286-92.
- 355 13. Mlczoch E, Brugger P, Ulm B, et al. Structural congenital brain disease in congenital heart
356 disease: Results from a fetal MRI program. *Eur J Paediatr Neurol*. 2012.
- 357 14. Clouchoux C, Kudelski D, Gholipour A, et al. Quantitative in vivo MRI measurement of
358 cortical development in the fetus. *Brain Struct Funct*. 2012;217(1):127-39.

- 1
2
3 359 15. Studholme C, Rousseau F. Quantifying and modelling tissue maturation in the living human
4 fetal brain. *Int J Dev Neurosci*. 2014;32:3-10.
5 360
6 361 16. Yushkevich PA, Piven J, Hazlett HC, et al. User-guided 3D active contour segmentation of
7 anatomical structures: significantly improved efficiency and reliability. *Neuroimage*.
8 362 2006;31(3):1116-28.
9 363
10 364 17. Namburete AI, Stebbing RV, Kemp B, Yaqub M, Papageorghiou AT, Alison Noble J.
11 Learning-based prediction of gestational age from ultrasound images of the fetal brain. *Med Image*
12 *Anal*. 2015;21(1):72-86.
13 365
14 366
15 367 18. van Velzen CL, Clur SA, Rijlaarsdam ME, et al. Prenatal diagnosis of congenital heart
16 defects: accuracy and discrepancies in a multicenter cohort. *Ultrasound Obstet Gynecol*.
17 368 2016;47(5):616-22.
18 369
19 370 19. Limperopoulos C, Tworetzky W, McElhinney DB, et al. Brain volume and metabolism in
20 fetuses with congenital heart disease: evaluation with quantitative magnetic resonance imaging and
21 spectroscopy. *Circulation*. 2010;121(1):26-33.
22 371
23 372
24 373 20. Dittrich H, Buhner C, Grimmer I, Dittrich S, Abdul-Khaliq H, Lange PE. Neurodevelopment
25 at 1 year of age in infants with congenital heart disease. *Heart*. 2003;89(4):436-41.
26 374
27 375 21. Zeng S, Zhou J, Peng Q, et al. Assessment by three-dimensional power Doppler ultrasound of
28 cerebral blood flow perfusion in fetuses with congenital heart disease. *Ultrasound Obstet Gynecol*.
29 376 2015;45(6):649-56.
30 377
31 378 22. Masoller N, Martinez JM, Gomez O, et al. Evidence of second-trimester changes in head
32 biometry and brain perfusion in fetuses with congenital heart disease. *Ultrasound Obstet Gynecol*.
33 379 2014;44(2):182-7.
34 380
35 381 23. Azpurua H, Alvarado A, Mayobre F, Salom T, Copel JA, Guevara-Zuloaga F. Metabolic
36 assessment of the brain using proton magnetic resonance spectroscopy in a growth-restricted human
37 fetus: case report. *Am J Perinatol*. 2008;25(5):305-9.
38 382
39 383 24. Alonso I, Borenstein M, Grant G, Narbona I, Azumendi G. Depth of brain fissures in normal
40 fetuses by prenatal ultrasound between 19 and 30 weeks of gestation. *Ultrasound Obstet Gynecol*.
41 384 2010;36(6):693-9.
42 385
43 386 25. Alves CM, Araujo Junior E, Nardoza LM, et al. Reference ranges for fetal brain fissure
44 development on 3-dimensional sonography in the multiplanar mode. *J Ultrasound Med*.
45 387 2013;32(2):269-77.
46 388
47 389 26. Wright R, Kyriakopoulou V, Ledig C, et al. Automatic quantification of normal cortical
48 folding patterns from fetal brain MRI. *Neuroimage*. 2014;91:21-32.
49 390
50 391 27. Miller SL, Huppi PS, Mallard C. The consequences of fetal growth restriction on brain
51 structure and neurodevelopmental outcome. *J Physiol*. 2016;594(4):807-23.
52 392
53 393
54
55
56
57
58
59
60

- 1
2
3 394 28. Griffiths PD, Bradburn M, Campbell MJ, et al. Use of MRI in the diagnosis of fetal brain
4 395 abnormalities in utero (MERIDIAN): a multicentre, prospective cohort study. *Lancet*.
5 396 2017;389(10068):538-46.
6
7 397 29. Kelly CJ, Makropoulos A, Cordero-Grande L, et al. Impaired development of the cerebral
8 398 cortex in infants with congenital heart disease is correlated to reduced cerebral oxygen delivery. *Sci*
9 399 *Rep*. 2017;7(1):15088.
10
11 400 30. Matthiesen NB, Henriksen TB, Gaynor JW, et al. Congenital Heart Defects and Indices of
12 401 Fetal Cerebral Growth in a Nationwide Cohort of 924,422 Liveborn Infants. *Circulation*. 2016.

13 402

14 403 **SUPPORTING INFORMATION legend**

15 404 Appendix S1. Description of the algorithm

16 405

17 406 **FIGURE LEGENDS**18 407 **Figure 1.** Schematic representation of a regression forest. Different brain regions are sampled
19 408 to calculate the brain-age in a 3D US volume

20 409

21 410 **Figure 2.** A visual representation of gestational age discriminating brain regions between 18-
22 411 32 weeks gestation. Colour scale is shown in the top left, top row: axial plane and bottom
23 412 row: coronal plane. The colours closest to 1.0 represent brain regions that are selected most
24 413 frequently by the algorithm.

25 414

26 415 **Figure 3.** Regression plot for 75 control cases: gestational age(‘true age’) on the x-axis and
27 416 age prediction on the y-axis.

28 417

29 418 **Figure 4.** The x-axis shows the gestational age at ultrasound(‘true age’), the y-axis shows age
30 419 as predicted by the algorithm. Legend: □ CHD cases, - - (interrupted line), ○ control cases.
31 420 — (continuous line).

32 421

422 **Table 1.** Baseline characteristics of included cases.

423

Characteristics	Value		Total
	CHD cases	Controls	
No. of women	90	75	
No. of analyzed volumes	199 (42%)	278 (58%)	477 (100%)
Characteristics			P-value
Maternal Age in years (Mean(SD))	29.76 (4.2)	32.08 (4.39)	0.30
BMI (kg/m ²) Mean(SD)	23.79 (4.2)	23.24 (3.8)	0.11
Primigravidae (%)	44 (42%)	25 (33%)	0.28
Diabetes n(%)	3(2.9%)	0(0%)	0.14
Total no. of CHD cases	90		n.a.
Major CHD			
HLHS	7		
Transposition of the Great Arteries	13		
Aortic Arch Hypoplasia and/or Aortic Stenosis	21		
Tricuspid or Pulmonary Atresia	11		
Tetralogy of Fallot or Fallot-like defect	15		
(un)balanced atrioventricular septal defect	7		
Other major CHD ^a	14		
Minor CHD			
Ventricular Septal defect	2		
Excluded Cases	14		n.a.

Fetal Intervention	3		
Postnatal non-isolated/syndromic	8		
Postnatal normal heart	3		
Pregnancy outcome			n.a.
Live birth	75 (83%)	75(100%)	
Termination of Pregnancy	15 (17%)	0(0%)	

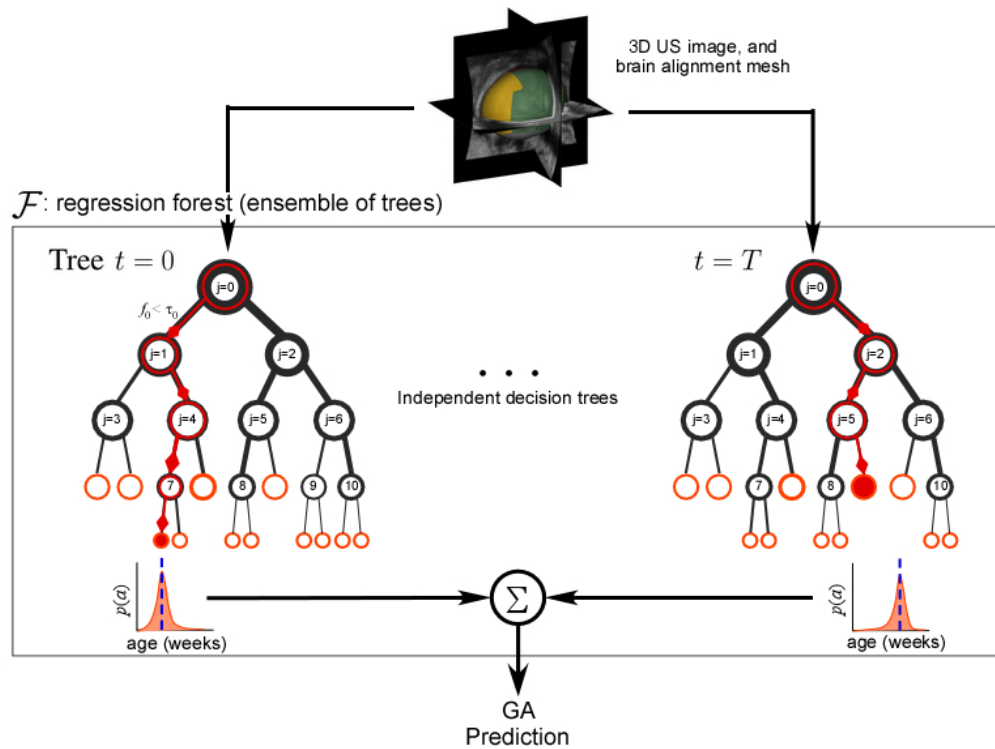
424 Abbreviations: CHD, Congenital Heart Defect; SD, Standard Deviation; BMI, Body Mass Index; HLHS,
 425 Hypoplastic Left Heart Syndrome; TGA, Transposition of the Great Arteries;

426 ^aOther major CHD include: Truncus Arteriosus, Multiple level left obstruction syndrome (Shone's complex),
 427 Double Outlet Right Ventricle-TGA, Congenitally Corrected TGA.

428

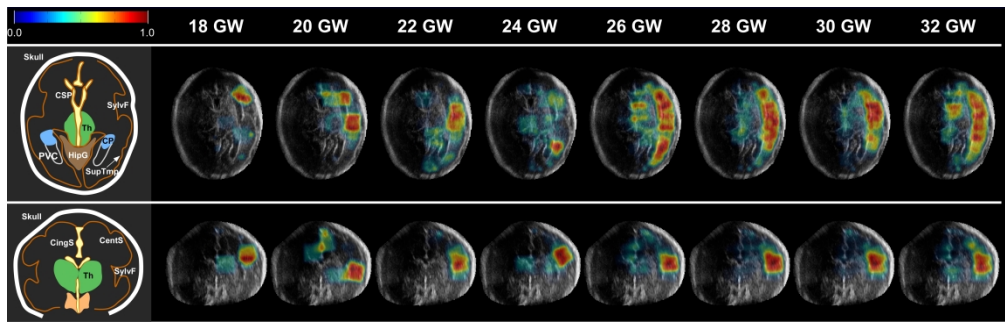
429

430



Schematic representation of a regression forest. Different brain regions are sampled to calculate the brain-age in a 3D US volume

1
2
3
4
5
6
7
8
9
10
11
12
13
14
15
16
17
18
19
20
21
22
23
24
25
26
27
28
29
30
31
32
33
34
35
36
37
38
39
40
41
42
43
44
45
46
47
48
49
50
51
52
53
54
55
56
57
58
59
60



A visual representation of gestational age discriminating brain regions between 18-32 weeks gestation. Colour scale is shown in the top left, top row: axial plane and bottom row: coronal plane. The colours closest to 1.0 represent brain regions that are selected most frequently by the algorithm.

1863x587mm (96 x 96 DPI)

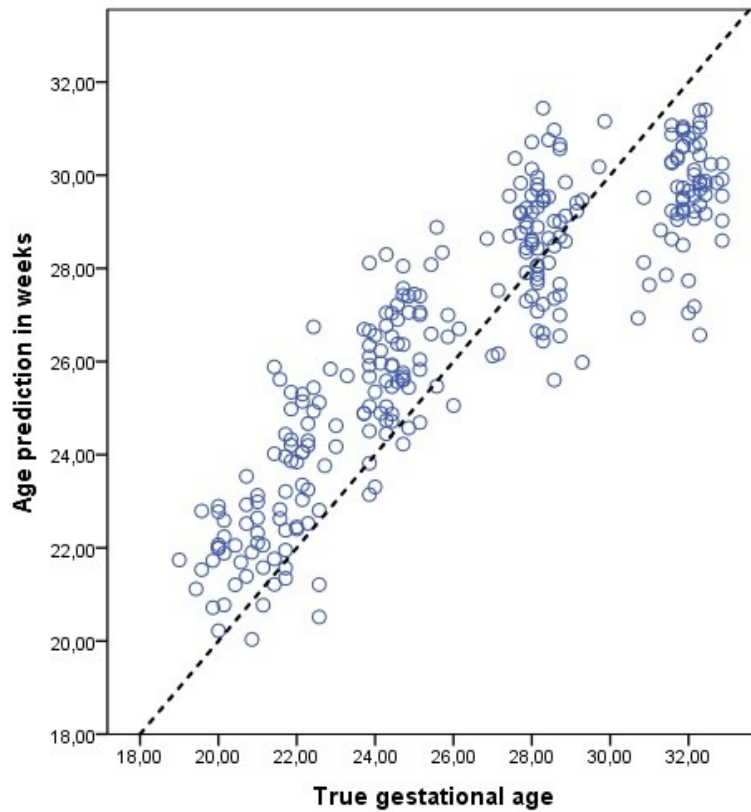


Figure 3. Regression plot for 75 control cases: gestational age('true age') on the x-axis and age prediction on the y-axis.

159x134mm (96 x 96 DPI)

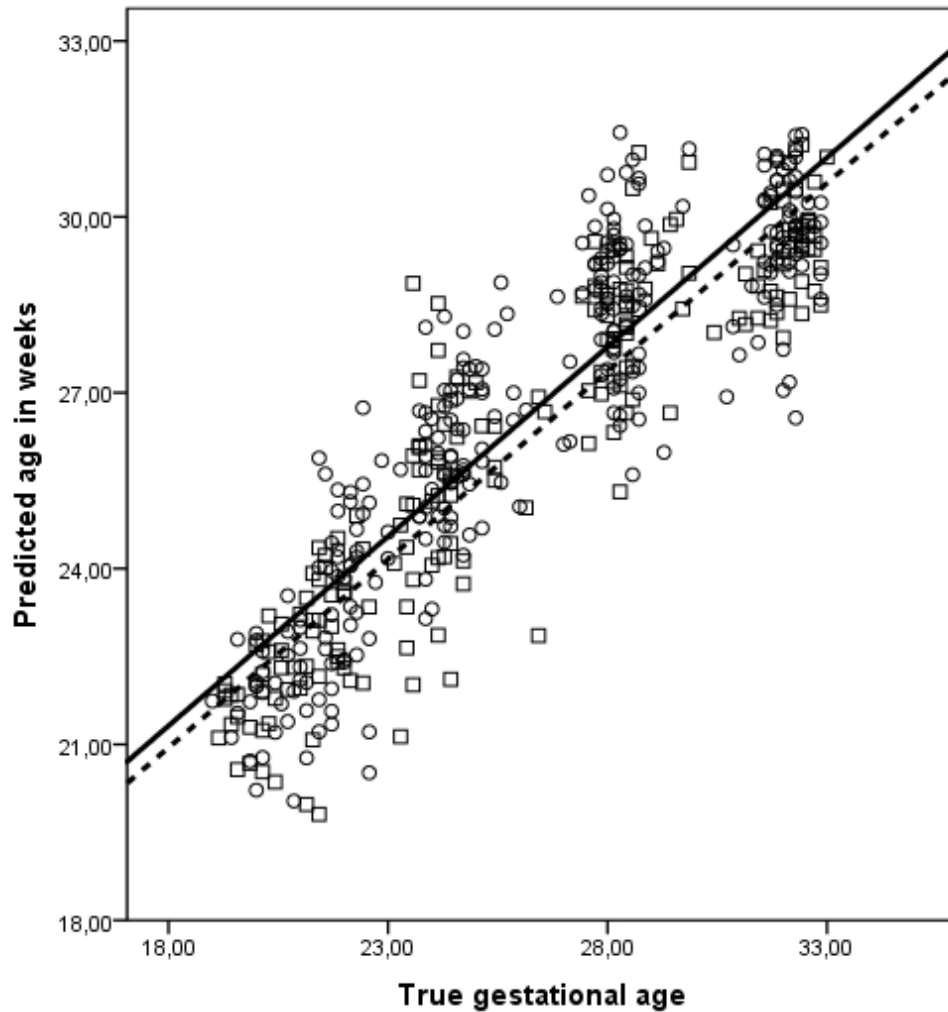


Figure 4. The x-axis shows the gestational age at ultrasound('true age'), the y-axis shows age as predicted by the algorithm. Legend: \square CHD cases, - - (interrupted line), \circ control cases. — (continuous line).

133x135mm (96 x 96 DPI)

Supplement

Estimation of gestational age is an essential part of safe obstetrical care. In order to provide an accurate age estimation, an ultrasonographic examination is performed around 10 weeks' gestation.

According to the 'ISUOG Practice Guideline: Performance of first-trimester fetal ultrasound scan': *Accurate dating provides valuable information for the optimal assessment of fetal growth and appropriate obstetric management. Dating a pregnancy by ultrasound between 10+0 and 13+6 weeks appears to be the most reliable method with which to establish true gestational age.*

The age prediction algorithm which we have used in a clinical group of CHD-fetuses, originates from the idea that not all women have access to a first-trimester ultrasound scan to accurately date their pregnancy. Especially women living in rural settings are at risk for erroneous obstetrical management, resulting from inaccuracies in gestational age.

The age prediction algorithm consists of an automated machine learning-based predictive model which has the ability to learn patterns of fetal brain changes over time. This model was 'trained' by 448 3D US images (GA range 18+0-33+6 weeks) from the INTERGROWTH-21st database (Papageorghiou et al. Lancet. 2014). This database contains a group of healthy volunteers from a low risk setting, for which pregnancy dating was performed following the ISUOG practice guideline as mentioned above. In addition, to account for natural variation in left and right hemispheres, only abdominal 3D Ultrasound(US) volumes were used with both visible hemispheres.

This supplement provides a more detailed description of the algorithm used in the main article.

Brain Feature Selection

Three-dimensional US volumes contain a large amount of information and possibly several neighbouring image patches containing similar information. Reducing the number of surface/image 'points' included in the search space reduces redundancy which in turn improves the computational cost. To this end, the cranial surface was densely evaluated with a pre-selected number of points to represent anatomical regions of interest, P (Figure S.1).

However, due to the effects of cranial calcification, the brain hemisphere proximal to the US probe is typically occluded, leaving only the distal hemisphere with visible and discernible intracranial structures. As such, feature extraction is confined to points on half of the cranial surface corresponding to the distal cerebral hemisphere in the image volume (Figure S.1). For simplicity, the surface is split by the midsagittal plane— defined by a normal vector and the centre point of the plane.

Appearance-Based Features

The appearance-based features used by the model comprise of two groups: sulcal and intracranial VOIs. Sulcal features are evaluated by affixing the VOI to the inner cranial surface (Figure S.2). They are designed to capture the sonographic image appearance related to changes in shape and morphology of the sulci and gyri on the cortical surface across gestation.

Intracranial features, on the other hand, are evaluated by displacing the VOI along the vector normal to Y^m (Figure S.1). For these features, the VOI can be placed anywhere in the trajectory between the inner skull and the falx cerebri (or midsagittal plane, Y^m). This ultimately covers the entire space in the cerebral hemisphere of choice.

Biometry-Based Features

Guided by prenatal assessment of fetal growth, the biometric feature is akin to the clinical head circumference (HC) measurement acquired from the standard transthalamic (TT) plane of the head. In this case, the feature is evaluated as the perimeter of the inner contour of the deformed cranial surface at the level of the diagnostic TT plane. The biometric HC feature captures global changes in head size in a manner similar to the current clinical method of GA estimation, emulating global (rigid) transformations related to fetal head growth.

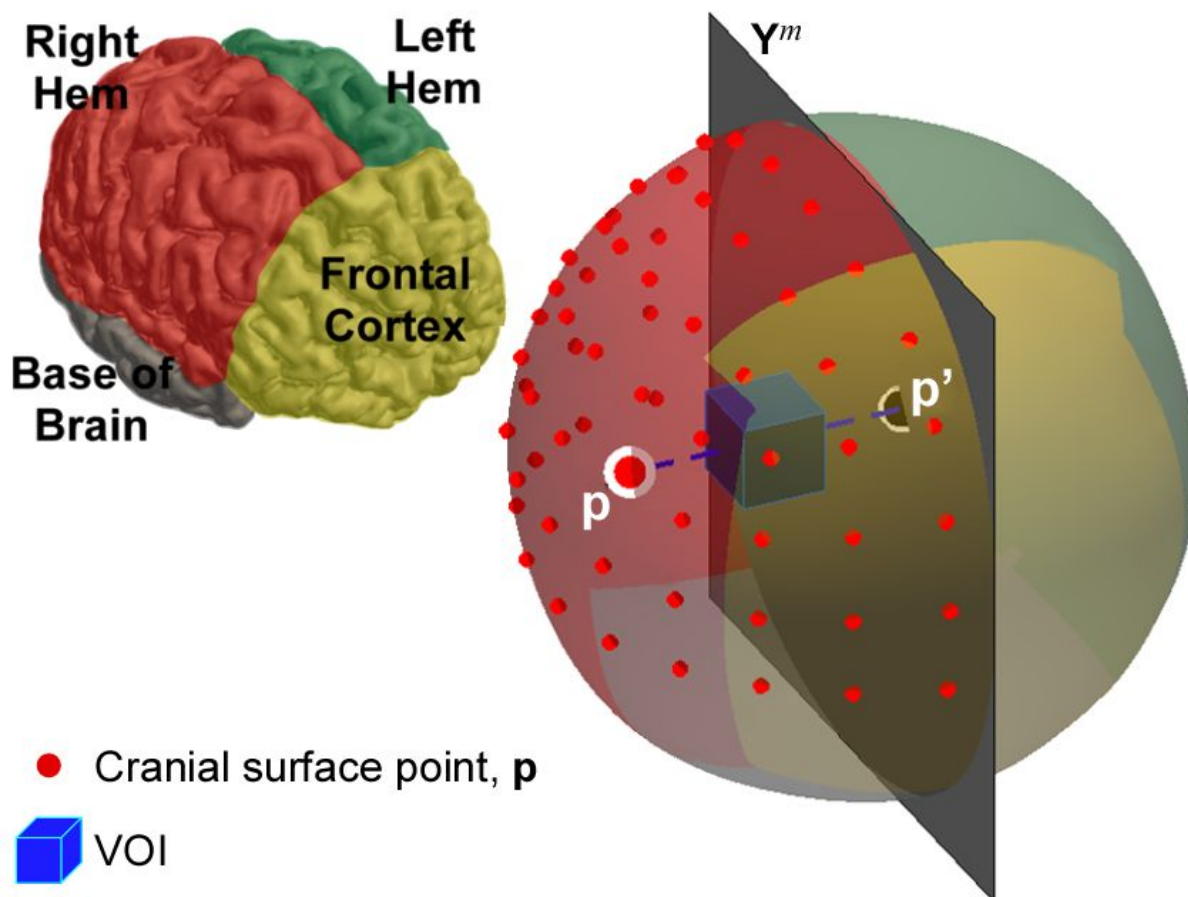


Figure S.1.

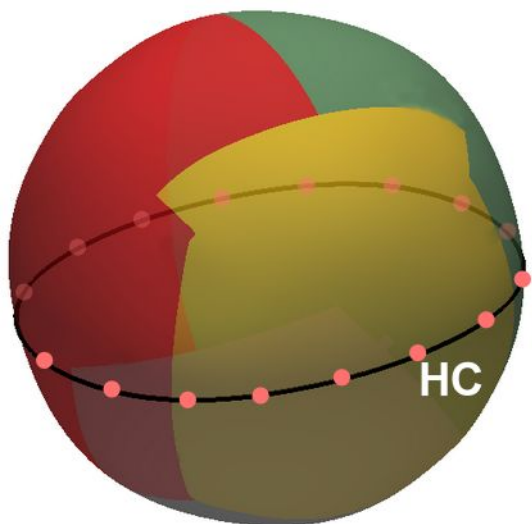


Figure S.2.

For Peer Review

GA Prediction

During age prediction, an unseen data sample (i.e. brain volume and corresponding surface) of unknown GA traverses the nodes in each tree of the trained forest model, and the binary test associated with each split node evaluates whether to send the data to the left or right child nodes, until the sample eventually reaches a leaf node (Figure S.3). For each tree, the leaf node reached provides a mean age estimate with an associated variance. Leaf nodes with high variance values have lower age certainty, so they are assumed to be less informative and likely to add noise to the output predictions. Therefore, a single prediction \bar{a} is generated by taking the mean of the GA estimated by all trees in the regression forest. Specifically:

$$\bar{a} = \sum_{t \in T} a_t$$

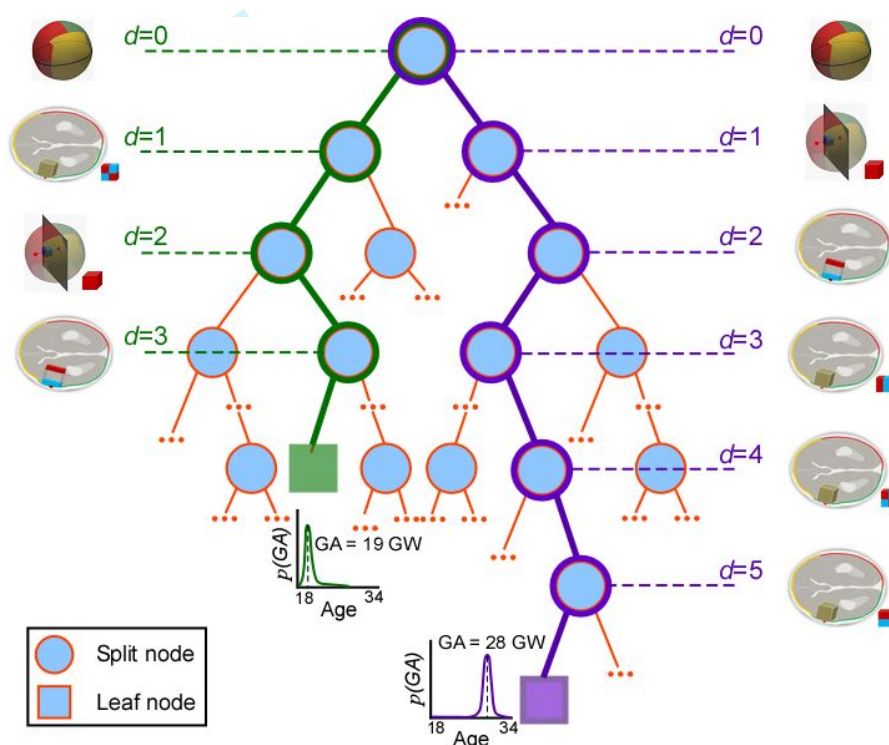


Fig S.3. GA Determination (Data used for model training)

In the INTERGROWTH-21st study, GA was defined by the known last menstrual period (LMP) and confirmed by a first-trimester (acquired between 9+0 and 13+6 GW) ultrasonographic measurement of the fetal crown-rump length. For added confidence, true GA was defined as the LMP- and CRL-based ages agreeing within 7 days, where the CRL-based GA is accurate within 2.7 days, as determined from 3 independent clinical measurements. All women included in the study were screened according to the INTERGROWTH-21st criteria and scanning protocol, and were thus identified as having low risk of impaired fetal growth and absence of fetal brain anomalies. Consequently, it was assumed that there were no delays in cortical development and that the fetal brains included in the study exhibited age-appropriate structural composition.

Image Selection for Model Training

Due to the fact that fetal head US images are typically challenged by reverberation artefacts (a consequence of increasing calcification of the cranial bones), the cerebral hemisphere proximal to the ultrasound probe is partially obstructed. Thus, the images selected for model training were included based on the following criteria:

1. Cranium occupies $\geq 50\%$ of the image
2. Distal cranial hemisphere is unobstructed
3. Interhemispheric fissure and falx cerebri are clearly visible in the entire supratentorial region
4. Sylvian fissure is visible in the distal hemisphere
5. Thalami are visible
6. Cavum septum pellucidum are visible

The images were converted to an isotropic spatial resolution whilst preserving anatomical boundaries, speckle, and texture profiles obtained during image acquisition.